RAPID COMMUNICATIONS

PHYSICAL REVIEW E VOLUME 47, NUMBER 4 APRIL 1993

Coupled phase instability of a cellular pattern

B. Janiaud,* H. Kokubo, and M. Sano

Research Institute of Electrical Communication, Tohoku University, Sendai 980, Japan

(Received 1 July 1992)

We have observed a localized structure and the spontaneous nucleation of topological defects in an experiment on electrohydrodynamic convection. They are created by a phase instability via the coupling between the oscillatory mode and the underlying cellular pattern. By measuring the coefficients of the phase equations derived from coupled complex Ginzburg-Landau equations, we have confirmed that the equations quantitatively describe the instability.

PACS number(s): 47.20.Ky, 05.45.+b, 47.65.+a

In many experimental systems driven out of equilibrium, such as Rayleigh-Bénard convection [1], directional solidification [2], and Taylor-Couette flow [3], the uniform state destabilizes into a spatially periodic pattern. The transition to spatiotemporal chaos in these systems is driven by secondary instabilities, which are responsible for the loss of spatial coherence as well as for the appearance of temporal complexity. Coullet and Iooss have predicted [4] that a remarkably rich variety of phenomena can emerge if the secondary instability couples with the underlying periodic pattern. However, this coupling has not been shown to exist in any earlier experiments.

In this Rapid Communication, we studied that the Hopf bifurcation of a periodic pattern in a convecting nematic liquid crystal leads to wave localization [target patterns, see Fig. 1(a)] and the spontaneous nucleation of dislocations. We show that the instability originates from the coupling between the oscillating mode and the underlying periodic pattern. We have determined the interactions based on coupled Ginzburg-Landau equations satisfying the symmetry properties of our system and on the derived coupled phase equations. We measure the coefficients of the phase equations and show that the equations quantitatively describe the instability.

Pattern formation by electrohydrodynamic (EHD) convection [5] in nematic liquid crystals has been studied as a prototype for spatiotemporal instabilities and chaos in large-aspect-ratio systems [6–9]. The advantage of EHD convection, compared to other systems, such as thermal convection, is that it has a short relaxation time scale and a large aspect ratio. These properties are essential for studying the long-time behavior of spatiotemporal chaos.

We used a nematic liquid crystal, 4-methoxybenzylidene-4′-butylaniline (MBBA) doped with 0.01 wt. % of tetra-*n*-butylammonium bromide to increase and control the electrical conductivity. It was sandwiched between two parallel glass plates covered with a transparent In_2O_3 electrode. The surface of the transparent electrodes was coated with polyvinyl alcohol and rubbed to achieve a uniform and unidirectional planar alignment of the nematic directors along the $\hat{\mathbf{x}}$ direction. The size of the cell was 2×2 cm^2 and its depth d_0 50 μm (aspect ratio 400 × 400). The temperature of the cell was regulated to (25.00± 0.01) °C. An ac voltage was applied between the two electrodes. Below the cutoff frequency of 900 Hz, due to the response time of the ions, the conduction state lost stability to a convective pattern, the Williams rolls. Further increasing the voltage, we observed a two-dimensional periodic grid pattern. Our typical working parameters were $f = 600$ Hz and $V = 58.6$ V. We observed the convection pattern under a microscope using a shadowgraph technique [10] with light polarized parallel to the nematic director. The intensity of the visualized image was measured with a charge coupled device camera and digitized with a resolution of 512×480 pixels and 256 grey levels. We used a complex demodulation method [11] to measure the local lattice wave number.

We focused on the dynamics of the grid pattern. When we crossed the boundary from a stationary state upward in the phase diagram shown in Fig. 1(b), the grid pattern underwent a Hopf bifurcation [12], oscillating in an optical mode [13]. In the oscillating region we observed a novel phenomenon [9, 12]; the oscillatory mode created waves that were emitted from a self-organized center and decayed outwards, defining a localized target pattern [see Fig. 1(a)]. The underlying periodic pattern (lattice) was locally expanded around the target's center. The targets have a life cycle, collapsing by the spontaneous nucleation of topological defects, to create spatiotemporal chaos.

To understand these phenomena, Ginzburg-Landau (GL) -type coupled equations based only on symmetry considerations are proposed. Our experimental observation indicated that the lattice spacing in the $\hat{\mathbf{x}}$ direction is deformed due to the interaction with the oscillations in the target, but spacing in the $\hat{\mathbf{y}}$ direction is not [12], implying that the oscillatory mode couples to the phase of the underlying periodic pattern only in the $\hat{\mathbf{x}}$ direction and not in the $\hat{\mathbf{y}}$ direction. Therefore we assumed that a one-dimensional model can explain the essential instability mechanism [14]. The basic periodic pattern (in the stationary regime) has parity symmetry, discrete translational symmetry, and time translational invariance. Based on these symmetry arguments the only possible normal forms for the complex coupled equations are [4]

$$\tau_A \partial_t A = \mu A + \xi_A^2 (1 + ic_1)\partial_x^2 A - (1 + ic_2)|A|^2 A + \xi_\phi (\xi_1 + i\xi_2)\partial_x \phi A, \quad (1)$$

$$\tau_\phi \partial_t \phi = \xi_\phi^2 \partial_x^2 \phi + \xi_A \delta \partial_x |A|^2 + i\xi_A \beta (\overline{A}\partial_x A - A\partial_x \overline{A}), \quad (2)$$

where all the coefficients are real. A represents the slowly varying amplitude of the wave (i.e., the target) and ϕ is the phase associated with the deformation of the underlying periodic pattern. τ_A (τ_ϕ) and ξ_A (ξ_ϕ) are the relaxation times and the coherence lengths of the wave A (the phase ϕ). Sakaguchi [15] predicted that the coupled instability could create either stationary or growing localized target patterns accompanied by lattice deformation. Furthermore, if lattice deformation (expansion or contraction) becomes large enough to exceed the Eckhaus boundary of the basic periodic pattern, spontaneous nucleation of defects is expected [12, 15].

Daviaud *et al.* [16] and Sakaguchi [15] derived coupled phase equations from Eqs. (1) and (2):

$$\partial_t \psi = D_\Psi \partial_x^2 \psi + \xi' k + \mathcal{N}, \quad (3)$$

$$\partial_t k = D_\phi \partial_x^2 k - \beta' \partial_x^2 \psi + \mathcal{N}, \quad (4)$$

where ψ is the phase of oscillatory mode A, k is the local wave number shift in the $\hat{\mathbf{x}}$ direction, $k = \partial\phi/\partial x$, and $\mathcal{N}$ denotes nonlinear terms. The coefficients are $D_\psi = (\xi_A^2/\tau_A)[1 + c_1 c_2 - (\tau_A \xi_\phi/\tau_\phi \xi_A) c_2 \beta \xi_1]$, $\xi' = \xi_\phi(\xi_2 - c_2\xi_1)/\tau_A$, $D_\phi = (\xi_\phi^2/\tau_\phi)[1 + (\xi_A/\xi_\phi)\delta\xi_1]$, and $\beta' = 2\mu\beta\xi_A/\tau_\phi$.

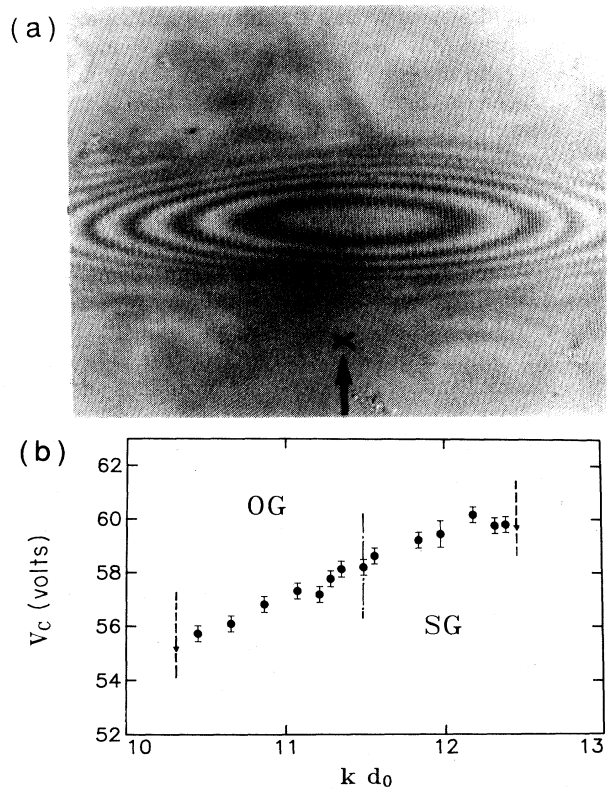

FIG. 1. (a) Snapshot of the shadowgraphic image of a target pattern created by the oscillation of an underlying two-dimensional cellular structure (lattice). (b) Phase diagram of the grid pattern as a function of the wave number and the voltage for $f = 600$ Hz. Bullets denote the threshold for the onset of oscillations. SG denotes the stationary grid pattern and OG the oscillating grid pattern. Dashed lines denote the Eckhaus boundary. Dotted-dashed line indicates the optimal wave number.

The uniform state is linearly unstable when $\beta'\xi'/D_\psi D_\phi > 0$. In this case, any small perturbation in the phase ψ is amplified in k and vice versa, leading to a coupled phase instability.

We performed different experiments to test the validity of the theory for our system. We chose experimental conditions where one term of the phase equations (diffusion or coupling) prevails on the other. This allows us to measure directly the values of the coefficients in the phase equations.

The coupling coefficient in Eq. (3) controls the variation of wave frequency with lattice wave number (see Fig. 2). We prepared a grid pattern with uniform initial lattice wave number k^i. By a frequency-voltage jump [8] to a state with a preferred wave number k^0, we generated oscillations of frequency shift $\omega = \partial_t \psi$. The slope of the linear fit (Fig. 2) gave $\xi' = (-0.48 \pm 0.05) d_0/T_0$, T_0 being the relaxation time of nematic director [17].

In order to determine the coefficient β', we measured the isophase line $\psi(x)$ and the local lattice wave-number shift $k(x)$ (see Fig. 3). The curve $\psi(x)$ was obtained by measuring the position of a wave front emitted from the center of a target. Since the oscillation period (of order T_0) was 10^3 times faster than the growth rate of $k(x)$ (see inset of Fig. 4), the local lattice wave-number shift $k(x)$ was quasistatic during the measurement of each isophase line. We measured the curvatures of the lattice wave number $\partial_x^2 k$ and of the oscillating phase $\partial_x^2 \psi$ for a growing target at each time step ($\Delta t = 10$ s), and found that they were proportional, as shown in Fig. 4. We checked that $\partial_t k$ is constant during the whole measurement (see inset in Fig. 4) and assumed that the nonlinear terms are negligible in Eq. (4). Thus, the linear fit in Fig. 4 gives the ratio of the two coefficients in Eq. (4): $D_\phi/\beta' = (-2.43 \pm 0.03) d_0$, giving (see the value of D_ϕ below) $\beta' = (-0.017 \pm 0.002) d_0/T_0$.

Let us consider the diffusion coefficients. We performed two different experiments to measure the diffusion coefficient of the lattice deformation, without waves, $D_\phi^0 \equiv \xi_\phi^2/\tau_\phi$, and with waves, D_ϕ. For D_ϕ^0, we prepared a pattern with a localized deformation: a target pattern was the most natural candidate. By stepping the voltage down to the stationary regime, we observed the relaxation of the lattice deformation without waves. At each time step ($\Delta t = 1$ s), we measured the value of the minimum wave number (the lattice constant is expanded in a target pattern) k_p and the width l at the half height of the peak. The product $k_p l$ was constant over a wide range (see the inset of Fig. 5), confirming that the undergoing process is a pure diffusion. The linear fit of the variation of k_p^{-2} with time (see Fig. 5) gives the diffusion coefficient without waves: $D_\phi^0 \equiv \xi_\phi^2/\tau_\phi = (4.2 \pm 0.7) \times 10^{-2} d_0^2/T_0$.

We evaluated the diffusion constant with waves from the data in Fig. 4. The extrapolation of the curve to the origin ($\partial_x^2 \psi = 0$) gives an estimate for the phase diffusion constant with waves, $D_\phi = (\xi_\phi^2/\tau_\phi)[1 + (\xi_A/\xi_\phi)\delta\xi_1] = 4.9 \times 10^{-2} d_0^2/T_0$. Comparing D_ϕ^0 and D_ϕ, we concluded

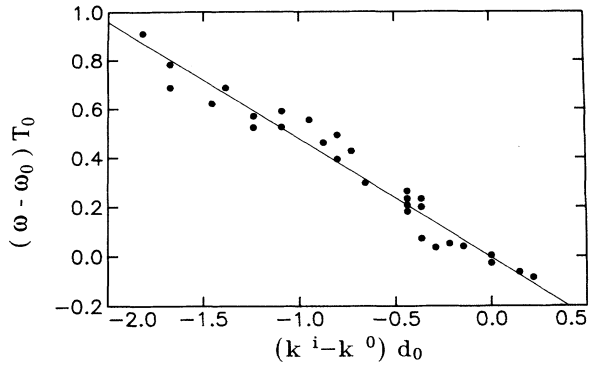

FIG. 2. The frequency of the phase wave mode vs the wave-number shift of the uniform grid pattern. The initial state of the basic grid pattern was controlled and the initial state of uniform k^i was varied by a frequency jump. The phase ψ of the wave is almost uniform in space. The Eckhaus instability finally takes over when the initial imposed wave-number shift is smaller than -1.2.

that the waves do not affect significantly the lattice diffusion constant. The instability mechanism lies in the coupling terms.

To estimate the wave diffusion constant D_ψ, we designed a cell with two separated plane electrodes; by applying different voltages in each region, we induced oscillations in one electrode and a stationary pattern in the other. We looked at the penetration of the wave into the stationary pattern. The phase contour $\psi(x)$ was parabolic and the wave-number shift k of the grid pattern was negligible in the penetrated region. From the measurement of the frequency and phase curvature relation based on Eq. (3), we found $D_\psi \simeq 0.71(d_0^2/T_0)$. Detailed explanations of the experimental setup will be published elsewhere [18].

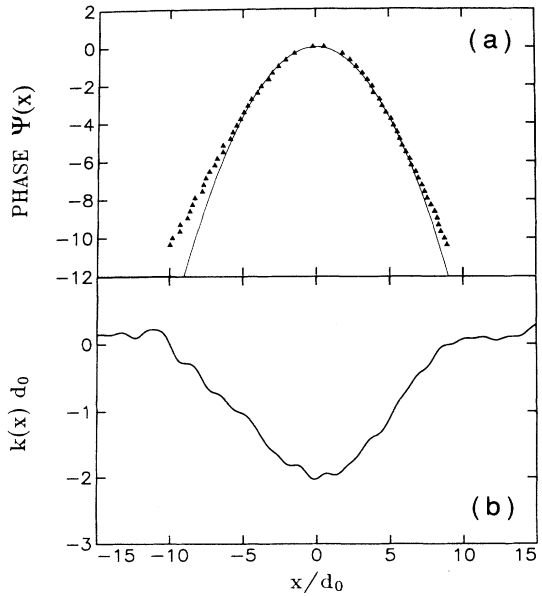

FIG. 3. (a) Isophase line $\psi(x)$ of the wave near the center of the target pattern. The solid curve indicates the best fit of the tip by a parabola. (b) Local wave-number shift $k(x)$.

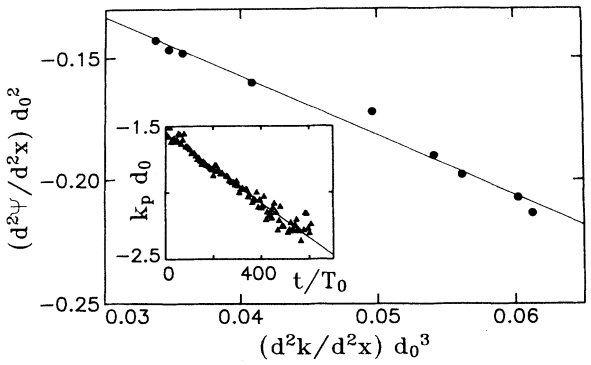

FIG. 4. Variation of the curvature of the phase wave ψ as a function of the curvature of the lattice wave number, k. The data were taken at the center of a growing target pattern. The linear slope gives the value of D_ϕ/β'. Inset: temporal evolution of the wave number k at the center of the target pattern.

We estimated the size of the nonlinear terms in Eq. (4) by evaluating the left-hand side (lhs) and linear terms in the rhs. They are about 10% of the value of the linear terms. Nonlinear terms in Eq. (3) give the deviation between the measured phase contour $\psi(x)$ and the parabolic solution. Near the center of the target, where we obtained the results shown in Figs. 4 and 5, the deviation was as small as the measurement error.

Comparing the experimental results and predictions [15], first, the instability condition $\beta'\xi' > 0$ (for $D_\psi D_\phi > 0$) is fulfilled, verifing our hypothesis that an amplifying feedback mechanism between the waves and the underlying lattice deformation creates the target pattern. In this case, $\beta' < 0$ and $\xi' < 0$, consistent with the observation that, at the center of the target pattern, the oscillation phase is advanced and the local wave number is smaller. If $\beta' > 0$ and $\xi' > 0$, the instability condition is satisfied, and the phase is also advanced, but the local wave number is larger rather than smaller.

Second, the directly measured growth rate of the target can be predicted by the considered phase equations. The growth rate, calculated by substituting the curvatures of k, ψ and our derived coefficients into the rhs of Eq. (4) is $\partial k/\partial t = (-1.2 \pm 0.3) \times 10^{-3}(1/d_0T_0)$. The growth rate

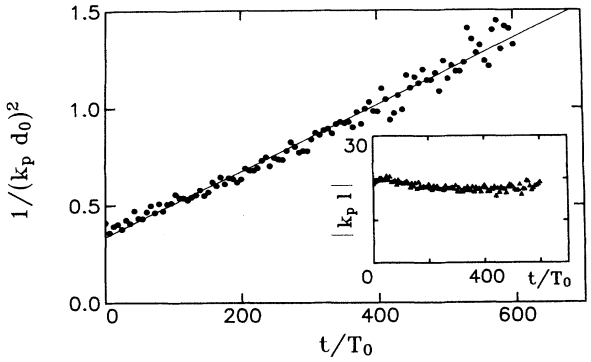

FIG. 5. Variation of minimum lattice wave number $(1/k_p^2)$ with time during a diffusion process after a jump in voltage. Inset: time evolution of the product $(k_p l)$.

directly measured from the slope of the inset in Fig. 4 is $(-1.3 \pm 0.1) \times 10^{-3}(1/d_0T_0)$, showing a good agreement. Furthermore, the contours of $k(x)$ and $\psi(x)$ in Fig. 3 are quite similar to those obtained by numerical simulations and to the analytic solution obtained by Sakaguchi [15].

This agreement supports the theory and validates the assumptions we have made for our measurements [14]. Nevertheless, for a further comparison between the experiment and the theory, we need to know the effect of the small nonlinear terms, such as $(\partial_x\psi)^2$, appearing in Eq. (3) [15, 16]. Studying the full amplitude equations, including nonlinear terms, should answer questions about the localized solutions and the defect nucleation process, and should lead to further experimental studies.

We are grateful to T. Kawagishi, S. Nasuno, and Y. Sawada for help and stimulating discussions; to P. Coullet, Y. Kuramoto, H. Sakaguchi, and S. Sasa for important insights; and to J. A. Glazier, A. Chiffaudel, J. M. Flesselles, T. Mizuguchi, and W. Zimmerman for useful comments. B. Janiaud thanks the Japanese Ministry of Education for financial support.

---

* Permanent address: Laboratoire de Physique Statistique, Ecole Normale Supérieure, 24 rue Lhomond, 75031 Paris CEDEX 05, France.

[1] L. Gil, G. Balzer, P. Coullet, M. Dubois, and P. Berge, Phys. Rev. Lett. **66**, 3249 (1991).

[2] J. M Flesselles, A. J Simon, and A. Libchaber, Adv. Phys. **40**, 1 (1991).

[3] C. D. Andereck, S. S. Liu, and H. L. Swinney, J. Fluid Mech. **164**, 155 (1986).

[4] P. Coullet and G. Iooss, Phys. Rev. Lett. **64**, 866 (1990).

[5] See, e.g., E. Bodenschatz, W. Zimmermann, and L. Krammer, J. Phys. (Paris) **49**, 1875 (1988), and references therein.

[6] S. Kai and K. Hirakawa, Prog. Theor. Phys. Suppl. **64**, 212 (1978).

[7] A. Joets and R. Ribbota, J. Phys. (Paris) **47**, 595 (1986).

[8] G. Goren, I. Procaccia, S. Rasenat, and V. Steinberg, Phys. Rev. Lett. **63**, 1237 (1989).

[9] S. Nasuno, M. Sano, and Y. Sawada, J. Phys. Soc. Jpn. **58**, 1875 (1989).

[10] K. Kondo, M. Arakawa, A. Fukuda, and E. Kuze, Jpn. J. Appl. Phys. **22**, 394 (1983).

[11] P. Bloomfield, *Fourier Analysis of Time Series: An Introduction* (Wiley, New York, 1976).

[12] M. Sano, K. Sato, S. Nasuno, and H. Kokubo, Phys. Rev. A **46**, 3540 (1992); M. Sano, K. Sato, and B. Janiaud, in *Pattern Formation in Complex Dissipative Systems,* edited by S. Kai (World Scientific, Singapore, 1992), p. 286.

[13] The regular grid pattern U_0 and its oscillatory mode u are well approximated by [12, 19]

$$U = U_0(x,y) + u(x,y,t) = S\cos(k_x x + \phi_x)\cos(k_y y + \phi_y) + A\cos(\omega t + \psi)\sin(k_x x + \phi_x)\sin(2k_y y + 2\phi_y).$$

The oscillatory mode u creating the target pattern is the second harmonic of the original grid pattern in the $\hat{\mathbf{y}}$ direction, but has the same wavelength in the $\hat{\mathbf{x}}$ direction. This oscillatory mode satisfies the orthogonality condition [4] with respect to the translational modes $\partial U_0/\partial x$ and $\partial U_0/\partial y$. In this paper we consider the equations for A, ψ, and $\phi \equiv \phi_x$.

[14] The target pattern looks like an ellipse because the expansion of the lattice in the $\hat{\mathbf{x}}$ direction (deformation of ϕ_x) is diffusing in the $\hat{\mathbf{y}}$ direction. We observed that the width of the target in the $\hat{\mathbf{y}}$ direction grows in time and finally the target becomes one dimensional (plane wave) when the target lasts long enough. This phenomenon and elliptic target pattern can be reproduced by an extended two-dimensional model simply by adding the term $\partial_y^2\phi_x$, i.e., diffusion of ϕ_x in the $\hat{\mathbf{y}}$ direction, to Eq. (2) or (4). However, the essence of the instability mechanism lies in the one-dimensional model.

[15] H. Sakaguchi, Prog. Theor. Phys. **87**, 241 (1992); **87**, 1049 (1992).

[16] F. Daviaud, J. Lega, P. Berge, P. Coullet, and M. Dubois, Physica **55D**, 287 (1992).

[17] We approximate the relaxation time T_0 of the nematic director by its value in zero electric field [5], $T_0 = Cd_0^2$, where C is determined by physical constants of MBBA. We thus estimate $T_0 = 165$ ms for the 50-μm cell.

[18] H. Kokubo, M. Sano, B. Janiaud, and Y. Sawada (unpublished).

[19] S. Sasa, T. Mizuguchi, and M. Sano, Europhys. Lett. **19**, 593 (1992).

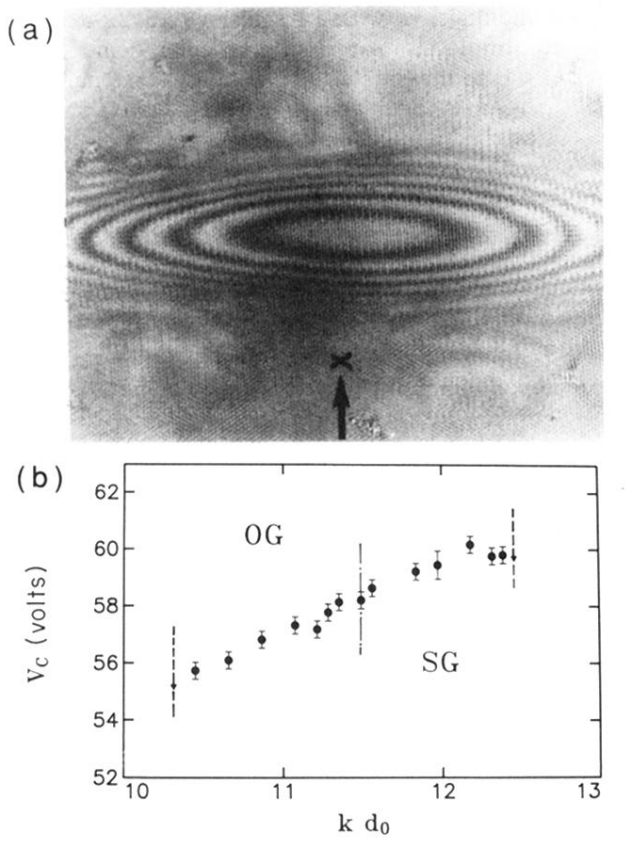

FIG. 1. (a) Snapshot of the shadowgraphic image of a target pattern created by the oscillation of an underlying two-dimensional cellular structure (lattice). (b) Phase diagram of the grid pattern as a function of the wave number and the voltage for $f = 600$ Hz. Bullets denote the threshold for the onset of oscillations. SG denotes the stationary grid pattern and OG the oscillating grid pattern. Dashed lines denote the Eckhaus boundary. Dotted-dashed line indicates the optimal wave number.